PHYSICAL REVIEW B, VOLUME 64, 041308(R)

Statistics of the domain-boundary relocation time in semiconductor superlattices

M. Rogozia,[1] S.W. Teitsworth,[2,*] H.T. Grahn,[1] and K.H. Ploog[1]
[1]*Paul-Drude-Institut für Festkörperelektronik, Hausvogteiplatz 5-7, 10117 Berlin, Germany*
[2]*Department of Physics, Duke University, Box 90305, Durham, North Carolina 27708-0305*
(Received 27 March 2001; published 3 July 2001)

Static domain formation in doped semiconductor superlattices results in several current branches separated by abrupt discontinuities that exhibit hysteresis. The transition from one branch to its adjacent one is studied by time-resolved switching experiments. The mean value of the relocation time increases by more than one order of magnitude, when the final voltage on the adjacent branch is reduced to a value approaching the discontinuity. At the same time, the distribution function of the relocation time changes from a simple Gaussian to a first-passage time form.

DOI: 10.1103/PhysRevB.64.041308 PACS number(s): 73.50.Fq, 73.40.Gk, 73.61.Ey

The current-voltage (I-V) characteristics of highly doped, weakly coupled superlattices (SL's) exhibit as many well-defined branches on each plateau as there are periods in the SL due to the formation of static electric-field domains.[1] Two branches are separated by a discontinuity in the current. In this case, the electric field inside the SL breaks up into two regions of constant field, which are separated by a domain boundary. The domain boundary is formed by a charge accumulation layer, which is basically confined to one SL period, i.e., to one quantum well of the SL. When the applied bias sweeps across a discontinuity from one current branch to the next, the domain boundary moves exactly by one SL period.[2] Recently, dynamical processes such as the domain formation time have been experimentally[3–5] and theoretically[6,7] studied. Previously, we found that for switching between two branches, the time constant of the response depends exponentially on the difference between the final current and the maximum or minimum current values, which is reached before the relocation of the domain boundary takes place.[5] The parameter for the exponential dependence is independent of the voltage pulse direction and number of branches involved in the relocation process. However, to our knowledge, the distribution of the switching times, which can give important information about the microscopic processes that determine the dynamics of switching, has not been investigated so far.

In this paper, we will determine the mean relocation time of the domain boundary and the relocation time distribution function in a weakly coupled SL. We concentrate on voltage jumps from one current branch to the adjacent one. As the final voltage approaches the voltage of the discontinuity from above, the mean switching time increases by more than one order of magnitude. At the same time, the distribution function changes from a Gaussian to a form, that closely fits a first-passage time distribution of the type one encounters in problems of Brownian motion.[8,9] The transition from one to the other distribution function appears to be universal even for voltage pulses covering several current jumps going to larger or smaller voltages.

The investigated sample consists of a 40-period SL with 9-nm-wide GaAs wells and 4-nm-wide AlAs barriers grown by molecular beam epitaxy. The central 5 nm of each well are Si doped with a density of 3×10^{17} cm^{-3}. The SL is sandwiched between two highly doped $Al_{0.5}Ga_{0.5}As$ contact layers in order to have access for optical measurements.[10] The sample is supplied with Ohmic contacts, etched into mesas with a diameter of 120 μm, and mounted on a sapphire holder in a He-flow cryostat equipped with 20-GHz coaxial cable. All reported measurements are performed at 5 K.

The time averaged I-V characteristics are recorded using a source-measure unit (Keithley SMU 236). In the experiments, we apply a negative voltage to the top contact of the sample. The square wave voltage pulses with a dc offset are generated using a pulse/function generator (Wavetek 81) with a width of 0.5 ms and a period of 1 ms. The pulse width and period are chosen to be sufficiently long to allow the field distribution inside the SL to stabilize after each voltage step in order to reset the field and charge distribution, before the next pulse arrives. The output of the generator is attenuated by 20 dB to increase the sensitivity of the amplitude steps of the generator. The current through the sample is amplified by 20 dB using the 50-Ω input of an amplifier (HMS model 571). Both the transients of the amplified current and the applied voltage are recorded at the 1-MΩ inputs of a real-time oscilloscope with a band width of 1 GHz (Lecroy LC 574 AL). The voltage signal is used as a trigger for the current transients of the voltage jumps. The current transient is either recorded directly or used for statistical measurements. We record the delay time τ_d of the current step after the voltage step (trigger) for up to 20 000 events and display the corresponding distribution function as a histogram.

The inset of Fig. 1 shows the I-V characteristics of the investigated sample at 5 K for two sweep directions, from 0 to -6 V (up sweep) and from -6 to 0 V (down sweep). The current plateau between -0.4 and -5 V originates from electric-field domain formation described in Refs. 1 and 11. For every current jump, the boundary between the high-field and low-field domain moves discontinuously from one quantum well to the adjacent one. In Fig. 1, an enlarged section of the I-V characteristics including the first five branches is depicted. The arrows indicate the sweep direction. The variation of the width of each branch has been shown to be mainly due to doping fluctuations in the

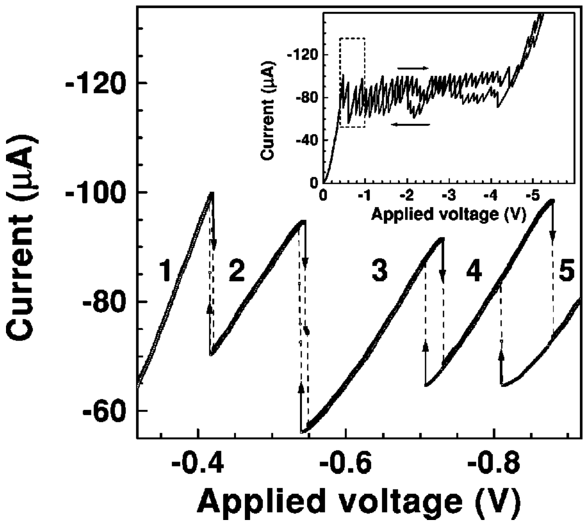

FIG. 1. Time-averaged *I*-*V* characteristics of the first five branches (1, 2, 3, 4, 5) for up sweep and down sweep between 0 and -6 V as indicated by the arrows at 5 K. The full *I*-*V* characteristics for both sweep directions is shown in the inset.

wells.[12–14] In this work we will focus on the switching times between the third and fourth current branch.

Typical time traces for switching from a fixed initial voltage on the third branch ($V_0 = -709$ mV) to several final voltages V_1 on the fourth branch are shown in Fig. 2. V_0 and the V_1 values labeled *A* to *F* are marked in the *I*-*V* characteristics in the inset. After switching the voltage, the current increases immediately to a value corresponding to the unstable part of the third branch, i.e., to a value, that can be reached by linear continuation of the third branch beyond the

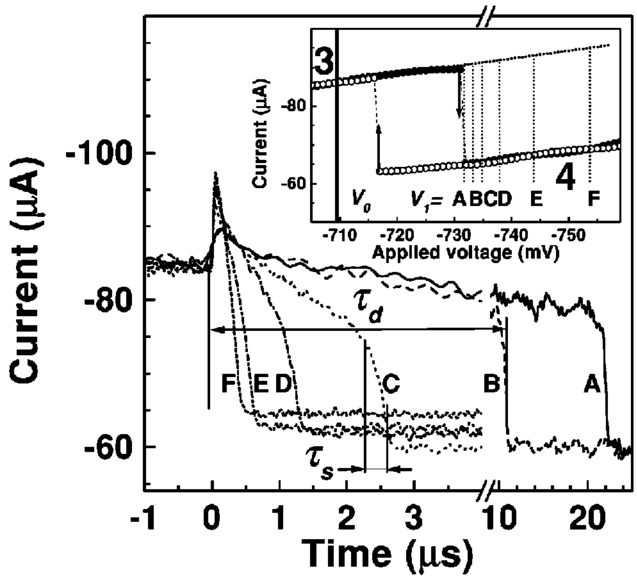

FIG. 2. Typical time traces for switching from V_0 on branch 3 to different voltages (*A* to *F*) on branch 4. The switching time τ is indicated for case *B*. The closer the final voltage is to the beginning of the fourth branch, the longer the switching time. The inset displays the time-averaged *I*-*V* characteristics indicating V_0 and the different final voltages V_1 labeled *A* to *F*.

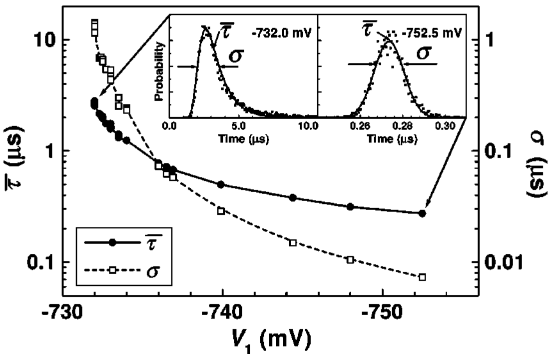

FIG. 3. Average value $\overline{\tau}$ (dots) and width σ (open squares) of the distribution of the relocation times for switching from $V_0 = -650$ mV on branch 3 to different final voltages on the branch 4. The insets show two examples of the distribution functions measured at a voltage of $V_1 = -732$ and -752.5 mV.

current jump. For large voltage jumps (cf. *F* in Fig. 2), the current reaches its final value on the fourth branch on a time scale of a few hundred nanoseconds. If V_1 is reduced approaching the voltage of the current jump for the up sweep, the current is almost constant (with a slight decrease) over a delay time τ_d, until it changes rapidly with a switching time τ_s. In fact, when the current value during τ_d falls below a critical level, the current switches to its final value. The switching time increases by a factor of 3.5 going from *F* to *A*. However, τ_d increases from 200 ns for large values of V_1 up to more than 20 μs for V_1 just above the current jump of the up sweep (*F* to *A* in Fig. 2).

In order to analyze the delay times in terms of their statistics, we have directly measured the distribution functions using the built-in functions of the oscilloscope. Two examples are shown as insets in Fig. 3. There is a very pronounced change in the shape of the distribution function going from larger to smaller values of $|V_1|$. The main part of Fig. 3 shows the averaged response times $\overline{\tau}$ (dots) and the respective widths σ (open squares) of the distributions on a logarithmic scale as a function of V_1. Both strongly increase with decreasing $|V_1|$ (*F* to *A* in Fig. 2). For values of V_1 far away from the current jump, the distribution function becomes very narrow (cf. inset for $V_1 = -752.5$ mV in Fig. 3) and exhibits a symmetric, Gaussian-like shape. However, for values of V_1 close to the current jump, the distribution function has a completely different, asymmetric shape with a steep increase at shorter times and a broad tail at longer times (cf. inset for $V_1 = -732.0$ mV in Fig. 3). Note that also the time scale has changed by more than one order of magnitude. The fits through the data points of the distribution functions will be discussed later.

In previous experiments,[3,4,6] the bias was changed from 0 V to its final value in order to study the formation of the domains, i.e., the boundary is moving over many SL periods. Here, we investigate the relocation of the domain boundary over a single period so that the domains are already formed by applying a finite bias V_0. However, in contrast to Ref. 5, we are now interested in the switching time distribution and its dependence on the final voltage V_1. Our results can be interpreted in the following way. When V_1 is located on the next higher branch, the domain boundary first remains in the same well. The current increases beyond the maximum of the initial branch of the *I*-*V* characteristic as seen in Fig. 2. Theoretical calculations by Carpio *et al.*[15] and Amann *et al.*[7] predict that for this current value the accumulation layer monopole can move against the flow of electrons, i.e., *upstream*. The field and charge profiles first begin to change without any spatial relocation of the charge accumulation layer itself. However, the center of mass of the total charge distribution moves upstream. During this time τ_d, the current remains almost constant. However, this intermediate state is metastable, because the center of mass of the charge distribution and the position of the charge accumulation layer are located in different wells of the SL. When the distance between the center of mass of the charge distribution and the accumulation layer reaches a critical value, the charge accumulation layer moves almost instantaneously to the adjacent well. The switching time τ_s can be estimated from current oscillation measurements, where the relocation of the domain boundary was observed as periodic spikes with a frequency of about 10 MHz.[16] Since the same sample exhibits current self-oscillations with spikes for the opposite polarity, a typical switching time should be of the order of 100 ns.

The time to reach this critical charge distribution depends on stochastic processes with a certain distribution, e.g., the uncertainty of the exact value of V_1 and scattering effects. For large voltage jumps, the change of the electric field distribution in the sample is relatively large so that the center of mass of the charge distribution is strongly accelerated and the critical charge distribution is only reached after a few stochastic processes. The resulting delay time τ_d is short and the corresponding time distribution symmetric and Gaussian. However, for values of V_1 close to the current jump, the field does not deviate very much from a stable distribution. At the same time, the center of mass of the charge distribution will be accelerated much less. Therefore, the system is expected to be much more sensitive to stochastic processes such as shot noise.[17] Hence, both the mean value of τ_d as well as the width of the time distribution increase. The current switches, when the critical charge distribution is reached *for the first time*. In fact, we consider a distribution function that describes the probability for a particle to reach $y=0$ starting from y_0 for the first time in a time between t and $t+dt$ by a random walk.[8] It is usually referred to as the first-passage time (FPT) distribution function. It is important to keep in mind that the variable *y* corresponds to the charge density in the quantum well associated with the domain wall.

After normalizing the measured time distributions (area equal to 1), we fit them at large values of V_1 with a Gaussian function of the form

$$W(t,\overline{\tau},\sigma)dt=\frac{1}{\sigma\sqrt{2\pi}}\exp\left(-\frac{(t-\overline{\tau})^2}{2\sigma^2}\right)dt, \qquad (1)$$

where $\overline{\tau}$ and σ denote the mean value and width, respectively, being the two parameters used in the fits. The resulting distribution function is shown in the inset of Fig. 3 for $V_1=-752.5$ mV. Note that a Gaussian would be expected, when there is an effective Brownian potential that has only one local minimum. The motion towards that minimum is essentially deterministic and fast.

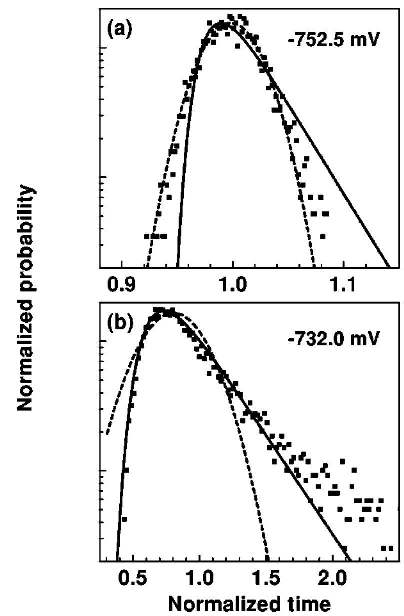

FIG. 4. Measured probability distribution functions fitted with a FPT (solid) and a Gaussian (dashed) distribution for the two final voltages (a) -752.5 mV and (b) $V_1=-732.0$ vs normalized time.

For small values of V_1 close to the current jump, we used the FPT distribution function of the form

$$W(t,y',\beta)dt=\sqrt{y'\frac{2\beta}{\pi}}\exp\left(-\frac{\beta}{2}y'z^2\right)dz \qquad (2)$$

with

$$y'=y_0^2/D \quad \text{and} \quad z=\frac{1}{\sqrt{\exp(2\beta t)-1}}. \qquad (3)$$

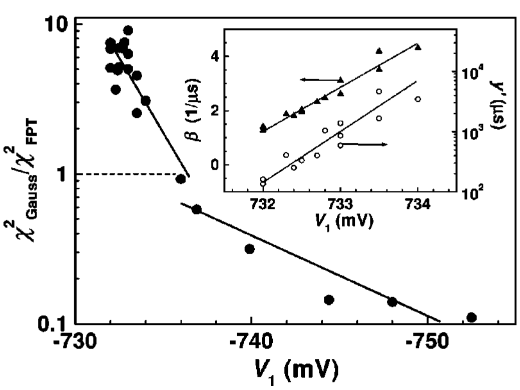

FIG. 5. Ratio of χ^2_{Gauss} to χ^2_{FPT} as a function of final voltage on branch 4. A transition happens at about 735 mV, where the ratio is about unity and the slope of the fitting line changes. The inset displays the dependence of the fitting parameters β (triangles) and y' (circles) on V_1 for the regime, where the above ratio is larger than one.

The parameters β and y_0^2/D are derived from the Fokker-Planck equation.[8,18] The resulting distribution function is asymmetric and contains a steep initial increase and a broad tail as shown in the inset of Fig. 3 for $V_1 = -732.0$ mV. Increasing β results in a narrower distribution, which at the same time is shifted to shorter times. An increase of y' mainly shifts the peak of the distribution to longer times in our parameter range.

For values of V_1 far away from the current jump, the distribution function is Gaussian as shown for $V_1 = -752.5$ mV (dashed line) in Fig. 4(a) on a semilogarithmic scale. The time scale is also normalized to the corresponding mean value. The distribution is very narrow. With decreasing values of V_1, the distribution becomes wider, but the distribution function still remains Gaussian. For $|V_1| < 735$ mV, the distribution function starts becoming more and more asymmetric developing a tail at longer times. The distribution function is not Gaussian anymore, but not FPT-like yet. With a further decrease of $|V_1|$, the distribution function approaches the FPT distribution (solid line) as shown in Fig. 4(b) for $V_1 = -732.0$ mV.

For each measured distribution, we calculated the quadratic deviation χ^2 from the respective least square fits. The ratio $\chi^2_{\text{Gauss}}/\chi^2_{\text{FPT}}$ describes which of the two distributions fits the data points better. Figure 5 shows the experimentally determined ratios for these distributions as a function of V_1. For $|V_1| < 735$ mV ($|V_1| > 735$ mV), the ratio is larger (smaller) than one, indicating that the FPT (Gaussian) distribution fits the measured distribution better. At the same time, the slope of $\log(\chi^2_{\text{Gauss}}/\chi^2_{\text{FPT}})$ changes significantly at $V_1 = -735$ mV. The inset of Fig. 5 shows the dependence of the two fitting parameters β and y' as a function of V_1 in the range where the distribution function is better described by a FPT distribution. Note the logarithmic scale for y'. Both parameters vary linearly with V_1 on the displayed scales.

In conclusion, we have investigated the relocation of the charge accumulation layer in a SL after a voltage pulse from the third to the fourth current branch. The mean delay time and the width of the distribution strongly increase, when the final voltage approaches the current jump from branch 3 to branch 4. At the same time, the distribution function of the delay time changes from a symmetric, Gaussian one to a very asymmetric, first-passage time one, indicating a fundamental shift in the switching dynamics as the transition is approached. Experiments for voltage pulses covering several current jumps and going to lower voltages reveal similar results for the time distribution, although the switching mechanism is changed from a monopole relocation to a dipole injection.

The authors would like to thank A. Fischer for sample growth and A. Amann and K. Matveev for stimulating discussions. One of us (S.W.T.) would like to thank the Paul Drude Institute for their hospitality. Partial support of the Deutsche Forschungsgemeinschaft within the framework of Sfb 296 is gratefully acknowledged.

*Electronic address: teitso@phy.duke.edu

[1] H.T. Grahn, R.J. Haug, W. Müller, and K. Ploog, Phys. Rev. Lett. **67**, 1618 (1991).

[2] L.L. Bonilla, in *Nonlinear Dynamics and Pattern Formation in Semiconductors and Devices*, edited by F. J. Niedernostheide (Springer-Verlag, Berlin, 1995), Chap. 1.

[3] J. Kastrup, F. Prengel, H.T. Grahn, K. Ploog, and E. Schöll, Phys. Rev. B **53**, 1502 (1996).

[4] Y. Shimada and K. Hirakawa, Jpn. J. Appl. Phys., Part 1 **36**, 1944 (1997).

[5] K.J. Luo, H.T. Grahn, and K.H. Ploog, Phys. Rev. B **57**, R6838 (1998).

[6] F. Prengel, A. Wacker, G. Schwarz, E. Schöll, J. Kastrup, and H.T. Grahn, Lith. J. Phys. **35**, 404 (1995).

[7] A. Amann, A. Wacker, L.L. Bonilla, and E. Schöll, Phys. Rev. E **63**, 066207 (2001).

[8] M.C. Wang and G.E. Uhlenbeck, Rev. Mod. Phys. **17**, 323 (1945).

[9] R.L. Stratonovich, *Topics in the Theory of Random Noise* (Gordon and Breach, New York, 1963), Vols. 1 and 2.

[10] H.T. Grahn, in *Semiconductor Superlattices* (World Scientific, Singapore, 1995), p. 160.

[11] J. Kastrup, H.T. Grahn, K.H. Ploog, F. Prengel, A. Wacker, and E. Schöll, Appl. Phys. Lett. **65**, 1808 (1994).

[12] A. Wacker, G. Schwarz, F. Prengel, E. Schöll, J. Kastrup, and H.T. Grahn, Phys. Rev. B **52**, 13 788 (1995).

[13] G. Schwarz, A. Wacker, F. Prengel, E. Schöll, J. Kastrup, H.T. Grahn, and K. Ploog, Semicond. Sci. Technol. **11**, 475 (1996).

[14] M. Patra, G. Schwarz, and E. Schöll, Phys. Rev. B **57**, 1824 (1998).

[15] A. Carpio, L.L. Bonilla, A. Wacker, and E. Schöll, Phys. Rev. E **61**, 4866 (2000).

[16] J.W. Kantelhardt, H.T. Grahn, K.H. Ploog, M. Moscoso, A. Perales, and L.L. Bonilla, Phys. Status Solidi B **204**, 500 (1997).

[17] Ya.M. Blanter and M. Büttiker, Phys. Rev. B **59**, 10 217 (1999).

[18] E.W. Montroll and B.J. West, in *Fluctuation Phenomena*, edited by E.W. Montroll and J.L. Lebowitz (North-Holland, New York, 1979), Chap. 2.